Electronic Supplementary Material (ESI) for ChemComm.


**Supporting information**

# Freeze-drying assisted biotemplated route to 3D mesoporous $Na_3V_2(PO_4)_3$@NC composites as cathodes with high performance for sodium-ion battery

Hongxia Sun, Zheng Liu, Fengyu Lai, Xiaodan Wang, Chao Wang, Nan Yu and Baoyou Geng*

*College of Chemistry and Materials Science, Anhui Key Laboratory of Functional Molecular Solids, Ministry of Education, The Key Laboratory of Electrochemical Clean Energy of Anhui Higher Education Institutes, Anhui Normal University, NO. 189 South Jiuhua Road, Wuhu, 241002, China.*

*Corresponding authors: Baoyou Geng (bygeng@mail.ahnu.edu.cn)*

**Experimental section**

Synthesis of NVP@NC composites: Sodium dihydrogen phosphate ($NaH_2PO_4$, AR, Aladdin), ammonium metavanadate ($NH_4VO_3$, AR, Aladdin) and oxalic acid dehydrate ($C_2H_2O_4{\cdot}2H_2O$, AR, Shanghai Lingfeng Chemical Reagent CO., LTD.), were used as starting reagents without further purification in the experiment. All fresh eggs were purchased from Supermarket (Wuhu, China). The separated egg white used as single solvent, carbon source and soft biotemplate during the synthesis. In the synthesis, 10 mmol $NH_4VO_3$ and 15 mmol $C_2H_2O_4{\cdot}2H_2O$ were added to egg white under magnetic stirring for 30 min at room temperature. Then, 15 mmol $NaH_2PO_4$ was dissolved in the above gelatinous mixture with continuous stirring for 30 min. During the procedure, the mixture filled up with air and got bigger. The preforms were obtained with a two-stage method: initially, the mixture were transferred into a refrigerator at -18 °C for pre-freezing for 12 h, subsequently, frozen mixture were freeze-dried (Labconco, Kansas, USA) under vacuum (0.018 mBar) at -60 °C for another 12 h. Eventually, the obtained preforms were annealed at 350 °C for 1 hour and 750 °C for 4 hours at the rate of 2 °C $min^{-1}$ under an Ar-5%$H_2$ flow to obtain the black 3D mesoporous NVP@NC composites. The prepared samples were denoted by the egg white content (7 mL, 8 mL and 9 mL) as NVP-7, NVP-8 and NVP-9. To further demonstrate the effect of the freeze-drying process, the contrast sample (NVP-8-H) was synthesized using the similar synthesis procedure of NVP-8 via normal drying process. The contrast samples (NVP-8-650, NVP-8-850) of NVP-8 also were prepared at different heated temperatures (650, 850$^{o}$C).

**Materials characterization**

The phase structures were characterized with X-ray powder diffraction (XRD, Bruker, D8 Advance). The surface morphologies of the samples were observed under scanning electron microscopy (SEM, Hitachi S-4800), the transmission electron microscopy (TEM, Hitachi, HT-7700), and the high-resolution transmission electron microscopy (HRTEM, FEI TECNAI-G2). The Raman scattering spectroscopy was performed with microscope confocal Raman spectrometer (Horiba Jobin Yvon, LabRAM HR800, France). The chemical state analysis was conducted by X-ray photoelectron spectroscopy (XPS, Thermo Fisher, ESCALAB 250XI). The relationship between mass and temperature was performed by thermal gravimetric analyzer (TA Corporation, TGA Q500, USA). Nitrogen adsorption−desorption was performed through Brunauer−Emmett−Teller (BET) method (Quantachrome Instruments, Quadrasorb EVO, USA).

**Electrochemical measurement**

The electrode slurry was prepared by mixing of 3D mesoporous NVP@NC active materials, conductive carbon black and polyvinylidene fluoride (PVDF) with a weight ratio of 8:1:1 in N-methyl-2-pyrrolidone solvent and then pasted on the aluminum foils with carbon coating. The as-prepared electrode was dried under vacuum at 100 $^{o}$C for 12 h. The electrodes were cut into disks with 12 mm diameters, and the average mass of the active materials of each electrode was about 1.5-2.0 mg. The electrode was assembled into CR2032 coin-type cells in an argon-filled glove-box. The sodium foils were used as the counter electrodes, and glass fibers were employed as the separators. The electrolyte was the solution of 1 M $NaClO_4$ in ethylene carbonate (EC)/ diethyl carbonate (DEC) (1:1, V/V) with 5% fluoroethylene carbonate (FEC). The coin cells with activated at room temperature for 12 h were measured using a Neware battery test system at a voltage window of 2.5-4.0 V. The cyclic voltammetry (CV) test and electrochemical impedance spectroscopy (EIS) spectra were performed on a CHI660E electrochemical workstation.

**Results**

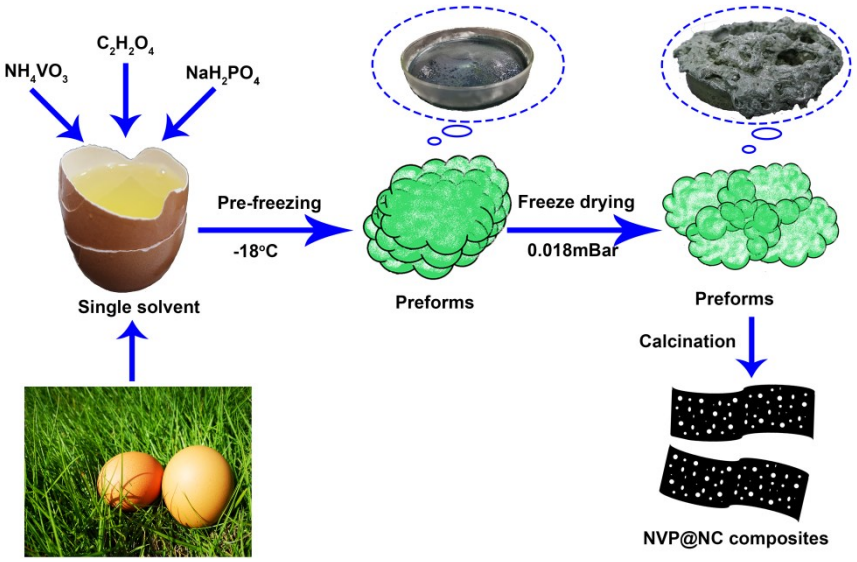


**Fig. S1** Schematic illustration of the formation of NVP@NC composites.

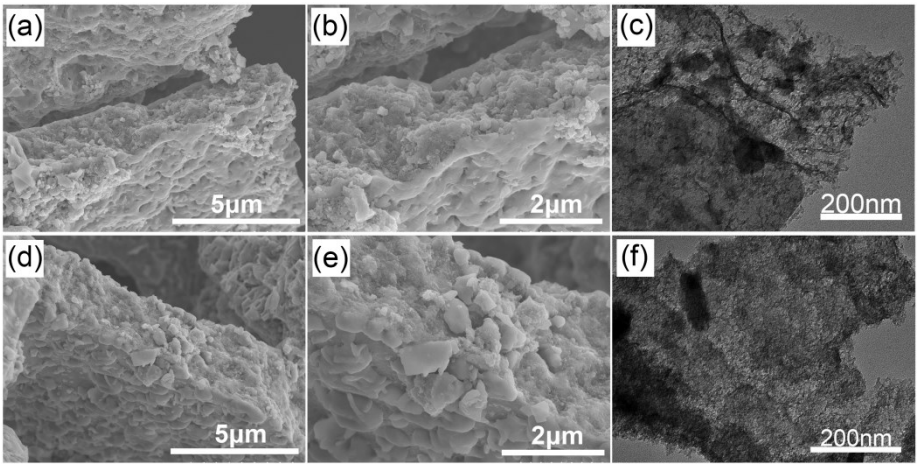


**Fig. S2** SEM images: NVP-7 (a-b), NVP-9 (d-e); TEM images: (c) NVP-7, (f) NVP-9.

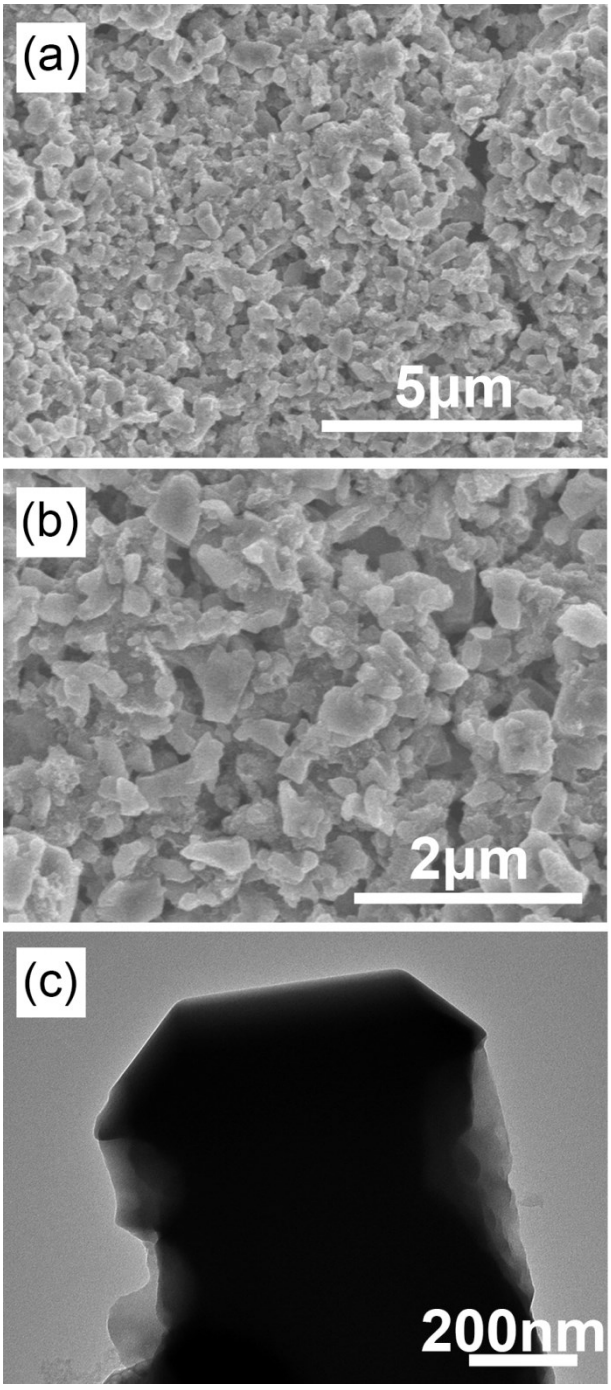


**Fig. S3** SEM images: Scale bar, 5μm (a), Scale bar, 2μm (b);TEM image (c) of NVP-8-H.

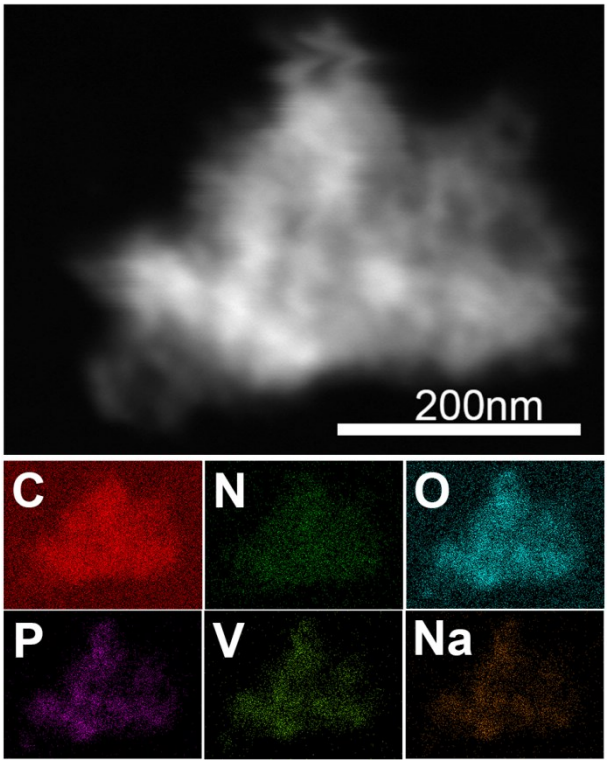


**Fig. S4** STEM image and corresponding elemental mapping images of NVP-8.

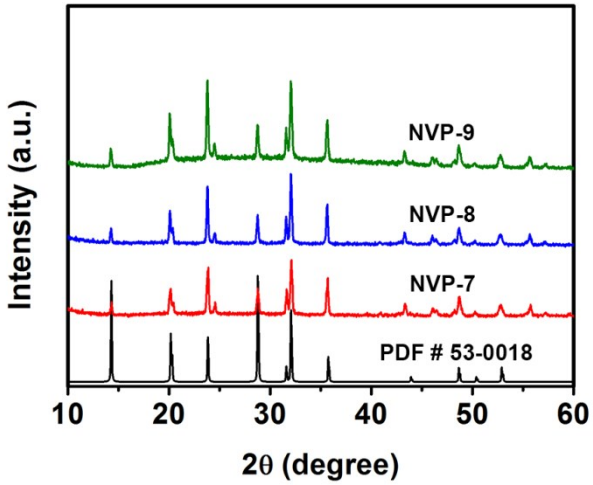


**Fig. S5** XRD patterns of NVP@NC composites.

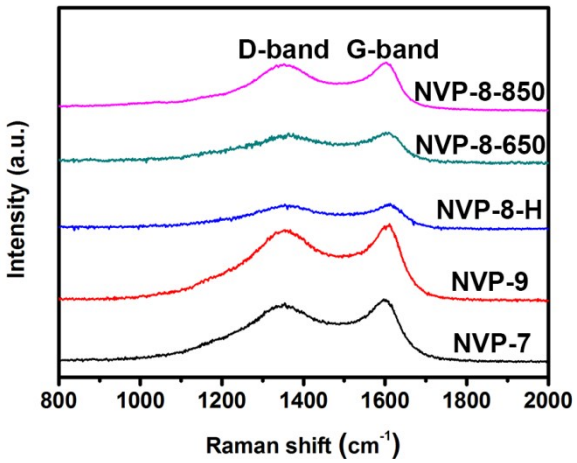


**Fig. S6** Raman spectra of NVP-7， NVP-9, NVP-8-H, NVP-8-650 and NVP-8-850.

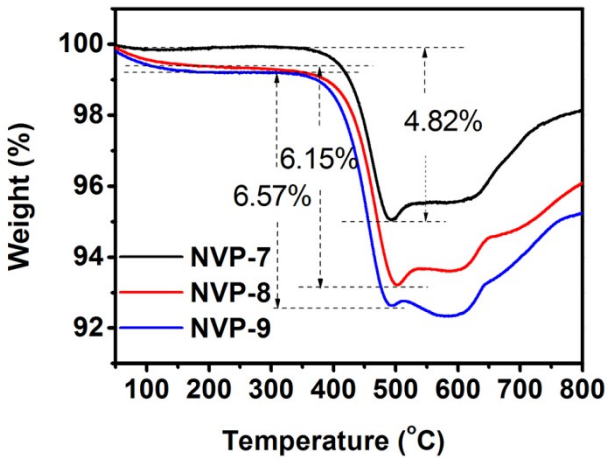


**Fig. S7** Thermogravimetric (TG) curves of NVP-7, NVP-8 and NVP-9.

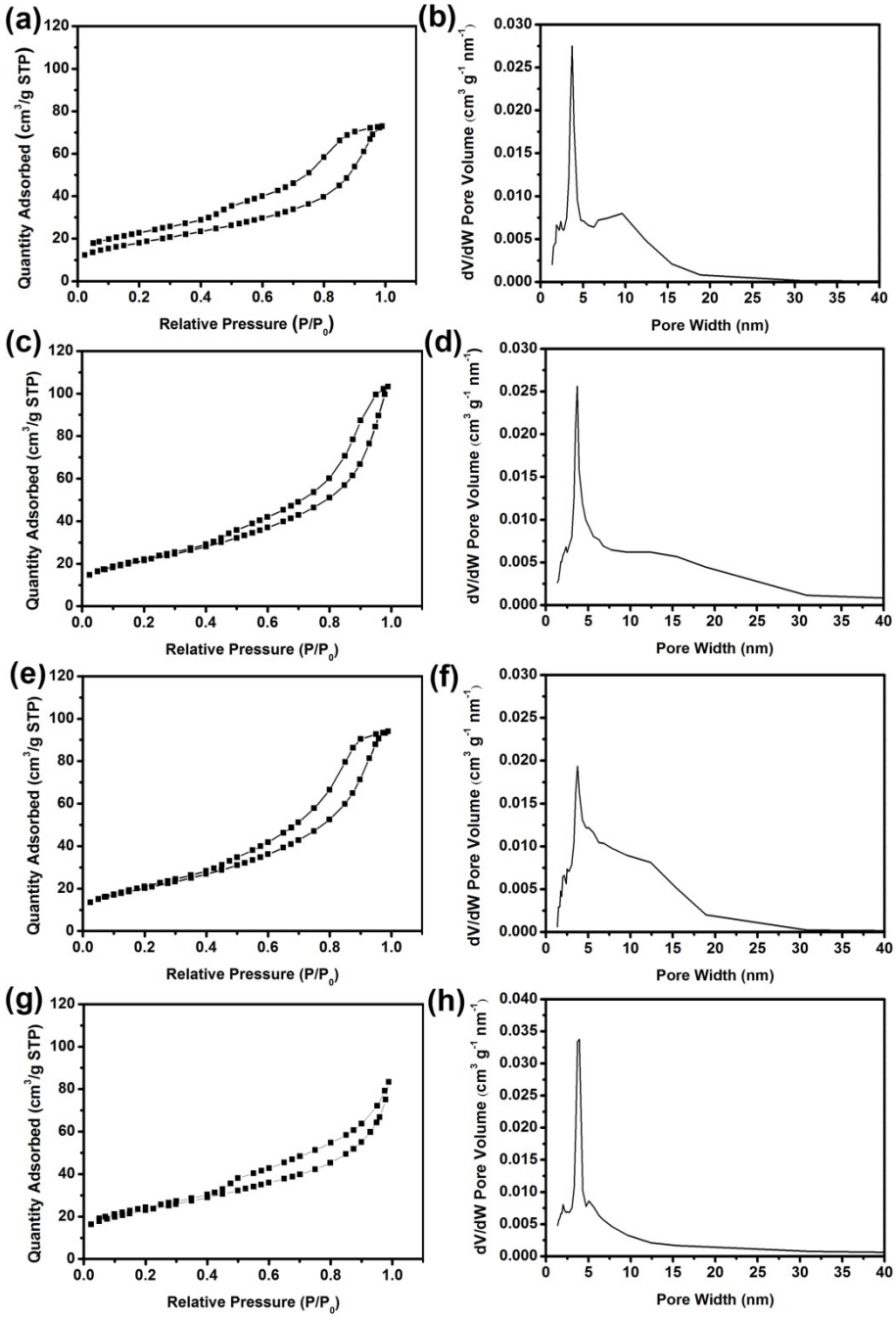


**Fig. S8** Nitrogen adsorption-desorption isotherms of NVP-7 (a), NVP-8 (c), NVP-9 (e), NVP-8-H (g); Pore diameter distributions of NVP-7 (b), NVP-8 (d), NVP-9 (f), NVP-8-H (h).

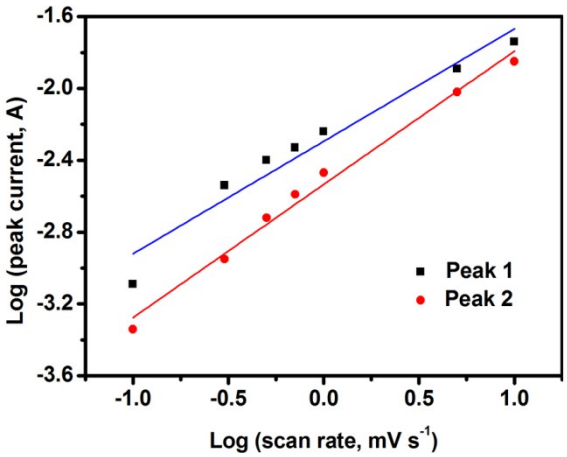


**Fig. S9** Log(current, A) *Versus* Log(scan rate, mV $S^{-1}$) plots at specific peak currents of NVP-8.

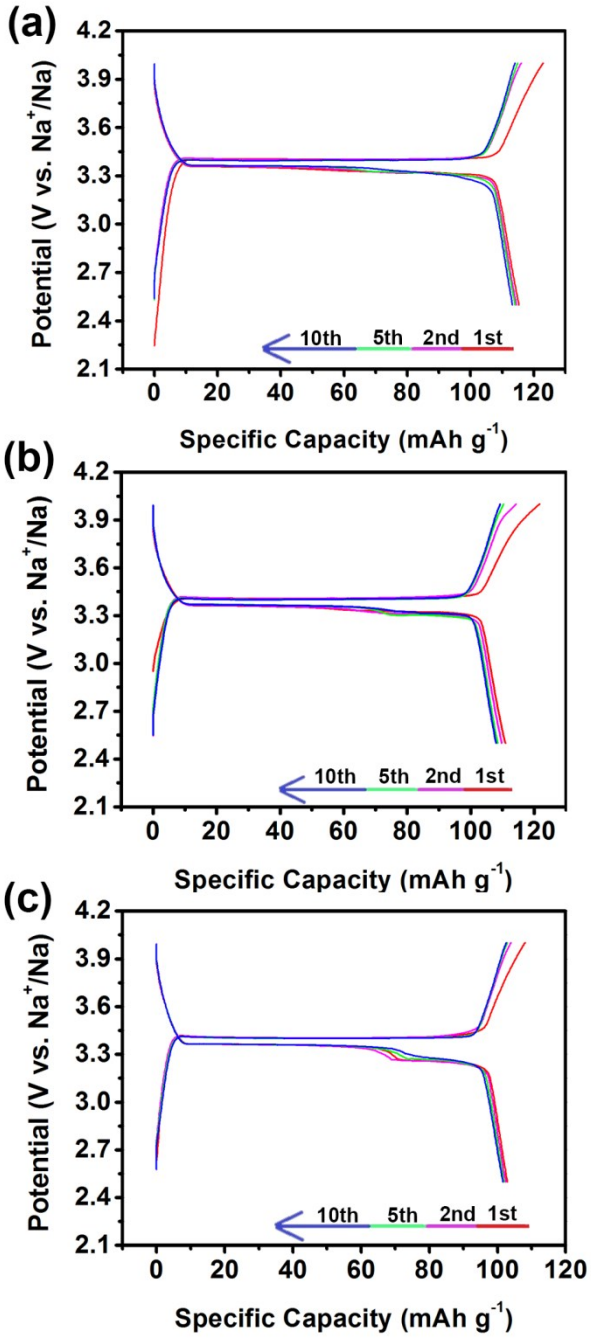


**Fig. S10** The charge-discharge capacities of NVP-7 (a), NVP-9 (b) and NVP-8-H (c) at 60mA $g^{-1}$.

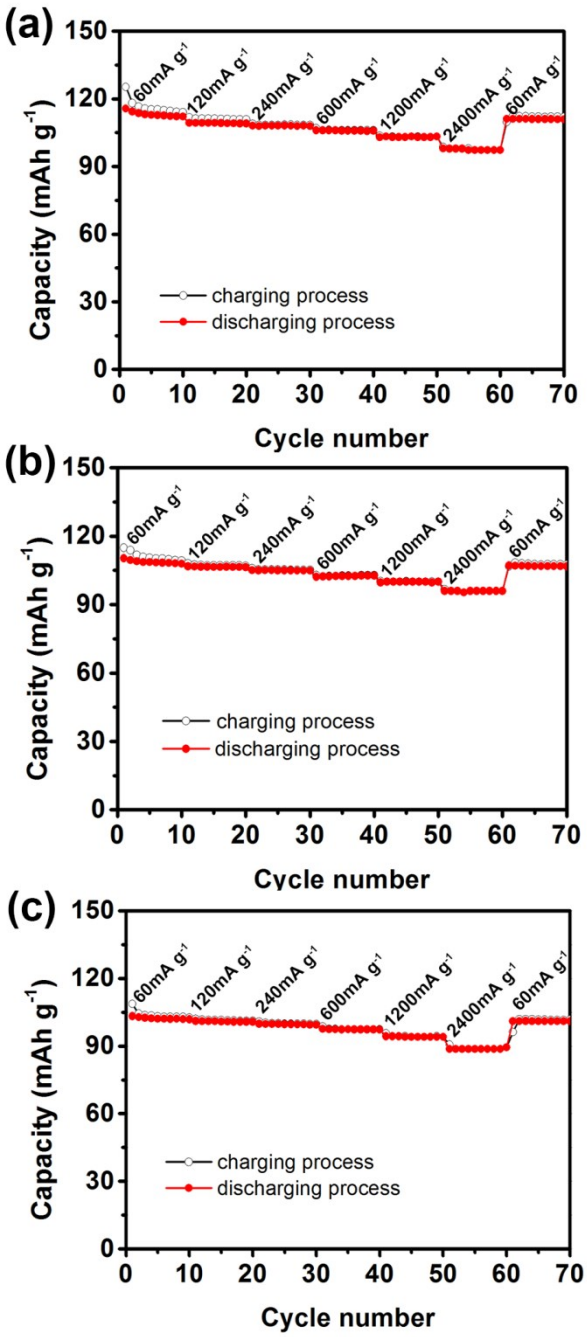


**Fig. S11** Rate performances of NVP-7 (a), NVP-9 (b), NVP-8-H (c).

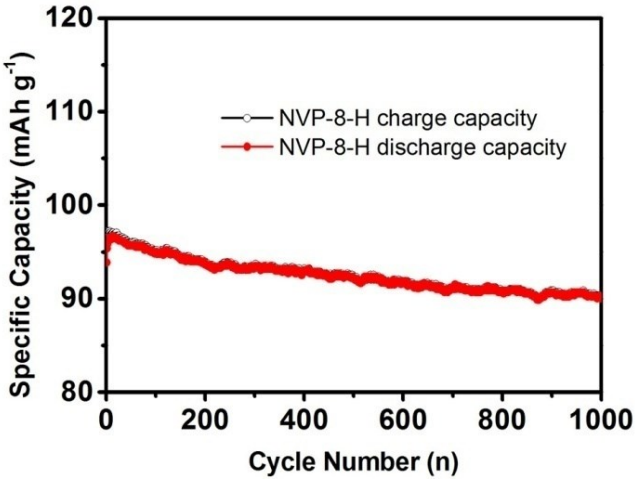


**Fig. S12** Cycling performance of NVP-8-H at 600 mA $g^{-1}$.

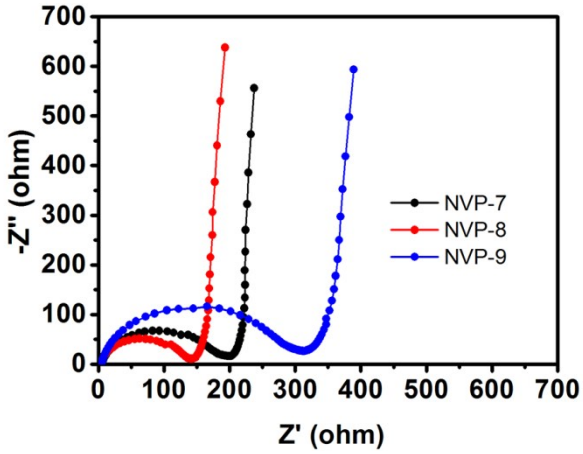


**Fig. S13** EIS curves of NVP-7, NVP-8, NVP-9.

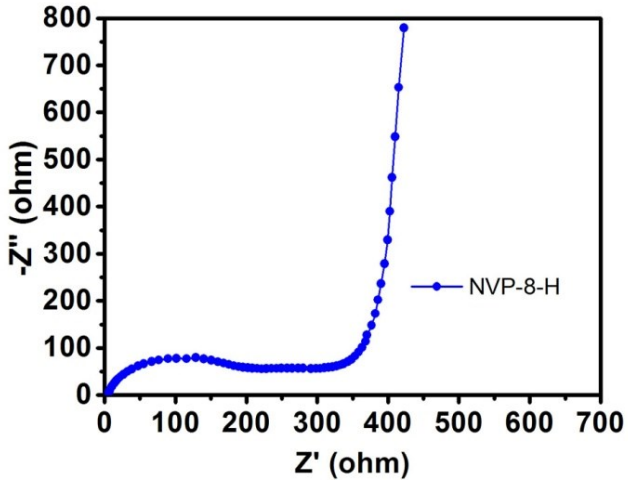


**Fig. S14** EIS curve of NVP-8-H.

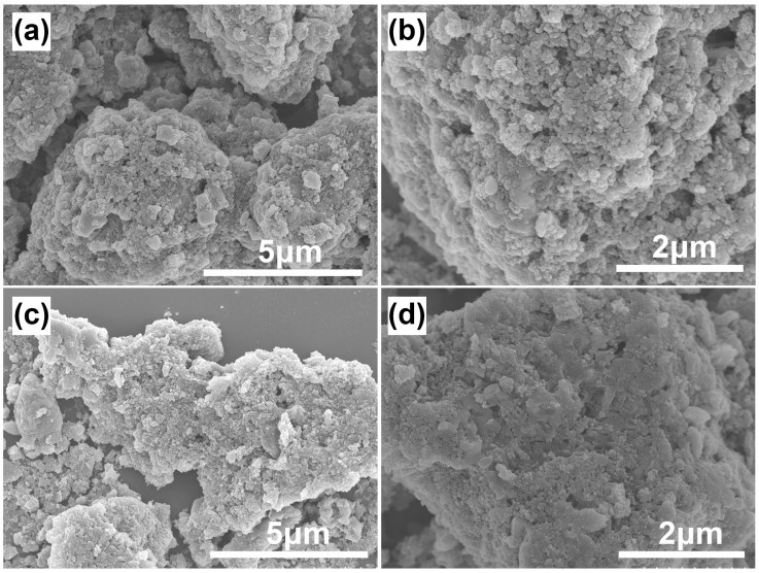


**Fig. S15** SEM images of NVP-8: before electrochemical test (a, b); after 1000 cycles at 60 mA $g^{-1}$ (c, d).

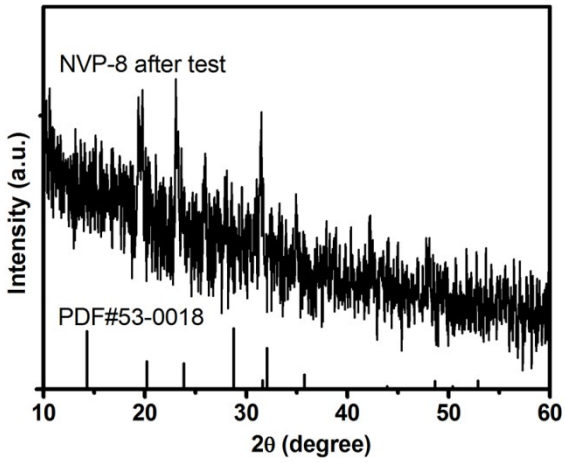


**Fig. S16** XRD of the tested NVP-8 .

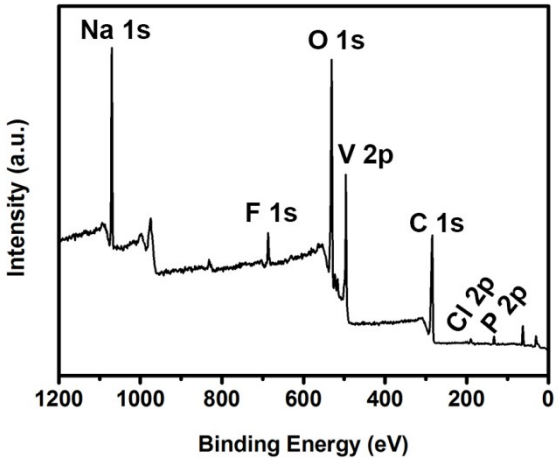


**Fig. S17** The XPS survey spectra of the tested NVP-8.

**Table S1** Comparison of the electrochemical performances of NVP-based composites as cathode for the SIBs

| Composite | Condition (voltage, conversion relation) | Discharge capacity | Cycling performance (capacity retention, rate, number of cycles) | Ref. |
|---|---|---|---|---|
| blackberry-shaped PC-NVP | 2.0-4.0 V; 1C=117mA $g^{-1}$ | 116, 111,107, 103, 96, 90 and 83 mAh $g^{-1}$ at 0.2, 0.5, 1, 2, 5, 10 and 20 C, respectively | 95.7%, 5C, 1000cycles; 95.1%, 10C, 4500 cycles | 1 |
| micro-size NVP/C | 2.0-4.0 V; 1C=117mA $g^{-1}$ | 106, 104, 101, 96, 89, 70 and 44 m Ah $g^{-1}$ at rates of 2, 5, 10, 20, 50, 100 and 200 C, respectively | 50%, 50C, 5000 cycles | 2 |
| NVP@rGo | 2.3-3.9 V; 1C=118mA $g^{-1}$ | 105.1, 104.6, 103.2, 103, 103.2, 101.6, 87.3, 84.1 and 79.2 mAh $g^{-1}$ at rates of 1, 2, 5, 10, 20, 50, 70, 80 and 100 C, respectively | 70%, 30C, 10000cycles | 3 |
| NVP/C-Ag-2 | 2.0-4.0 V; ---- | 114.9, 108.3, 95 and 86.5 mAh $g^{-1}$ at rates of 0.2, 1, 10 and 50C, respectively | 97.5%, 10C, 500 cycles | 4 |
| NVP-M2 | 2.3-3.9 V; 1C=117.6 mA $g^{-1}$ | 114.8, 111.4, 109.4, 109.2, 106.8, 104.6, 95.2, 71.6 mAh $g^{-1}$ at rates of 0.1, 0.2, 0.5, 1, 3, 5, 10 and 20C, respectively | 84.4%, 1C, 500 cycles; 93.5%, 5C, 300 cycles | 5 |
| NVP/C-MSs | 2.5-4.0 V; 1C=117.6mA $g^{-1}$ | 116.3,114.7,109.8 mAh $g^{-1}$ at 0.5, 1 and 10 C respectively | 94.7%, 1C, 1000cycles; 91.9%, 5C, 1000cycles; | 6 |
| NVP-Freestanding | 2.5-4.0 V; 1C=117mA $g^{-1}$ | 116,103, 97, 92, 84, 78 and 71mAh $g^{-1}$ at 0.1, 0.5, 1, 2, 5, 10 and 20 C respectively | 88.6%, 0.5C, 150cycles; | 7 |
| NVP@NC | 2.5-4.0 V; 1C=120mA $g^{-1}$ | 117, 114.7,108.8, 106.1, 103.1 and 100.0 mAh $g^{-1}$ at 0.5, 1, 2, 5, 10 and 20 C respectively | 95.8%, 5C, 1000cycles; 93.9%, 20C, 1000cycles | This work |

**References**


1. J. Zhang, W. Liu, H. Hu, X. Li, Y. Huang, T. Chen, Y. Zhuo and K. Liu, Electrochimica Acta, 2018, 292, 736-741.

2. J. Yang, D. Li, X. Wang, X. Zhang, J. Xu and J. Chen, Energy Storage Materials 2020, 24, 694–699.

3. F. Li, Y. Zhu, J. Sheng, L. Yang, Y. Zhang and Z. Zhou, J. Mater. Chem. A, 2017, 5, 25276.

4. X. Hong, X. Huang, Y. Ren, H. Wang, X. Ding and J. Jin, Journal of Alloys and Compounds 2020, 822, 153587.

5. X. Liu, G. Feng, Z. Wu, D. Wang, C. Wu, L. Yang, W. Xiang, Y. Chen, X. Guo and B. Zhong, Journal of Alloys and Compounds 2020, 815, 152430.

6. X. Cao, A. Pan, B. Yin, G. Fang, Y. Wang, X. Kong,T. Zhu, J. Zhou and G. Cao, S. Liang, Nano Energy 2019, 60, 312–323.

7. Q. Ni, Y. Bai, Y. Li, L. Ling, L. Li, G. Chen, Z. Wang, H. Ren, F. Wu and C. Wu, Small, 2018, 14, 1702864.